Potential energies and cross sections for MgH^+

R. E. Olson
Molecular Physics Laboratory, SRI International, Menlo Park, California 94025

B. Liu
IBM Research Laboratory, San Jose, California 95193

(Received 13 March 1979)

Configuration-interaction (CI) potential curves have been calculated for the ten lowest singlet molecular states of MgH^+. The $X\,^1\Sigma$, $A\,^1\Sigma$, and $B\,^1\Pi$ molecular states are calculated to be bound by 1.93, 1.93, and 0.18 eV at equilibrium separations 3.16, 3.84, and $4.41a_0$, respectively. These potential-well characteristics are in reasonable accord with analyses performed on spectroscopic data. The CI potential curves were employed in a three-channel scattering calculation to estimate $H^+ + Mg$ electron-capture cross sections at velocities $(0.1\text{–}1.4) \times 10^8$ cm/sec. Capture with excitation of the ion dominates with $H + Mg^+$ $(3p)$ being the major electron-capture channel at 1×10^8 cm/sec. At higher velocities, a classical-trajectory Monte-Carlo method was used to calculate both the electron-capture and impact-ionization across sections for the $H^+ + Mg$ collision pair. The calculated electron-capture cross sections are in reasonable agreement with the recent measurements of Morgan and Eriksen.

I. INTRODUCTION

Recently, there has been interest in measuring the single- and double-electron-capture cross sections for collisions of protons with magnesium.[1,2] This work is of both applied and fundamental interest. The cross sections are useful in the development of ion sources to produce intense beams of H^- for heating and fueling tokamak plasmas. On the fundamental side, it is of interest to understand the mechanism for electron capture in collisions of protons with magnesium,

$$H^+ + Mg \rightarrow H + Mg^+ . \tag{1}$$

In particular, a Mg-atom target is a convenient prototype for understanding electron capture by protons from the alkaline-earth series.

To be able to calculate the low-energy cross sections for (1), it is first necessary to determine the singlet molecular curves arising from the low-lying states of MgH^+ ($H^+ + Mg$ is the second excited $^1\Sigma$ state of MgH^+). These curves allow us to estimate the cross sections and also shed light on the collision pathways for the double-electron-capture process

$$H^+ + Mg \rightarrow H^- + Mg^{2+} , \tag{2}$$

which previously was proposed to be especially efficient in this system.[3]

Also, we have applied the classical-trajectory Monte Carlo method to the $H^+ + Mg$ collision system to calculate the high-energy ($E \gtrsim 10$ keV) electron-capture cross sections for (1), and the impact-ionization cross sections for

$$H^+ + Mg \rightarrow H^+ + Mg^+ + e . \tag{3}$$

The calculated cross sections are compared with experimental data to assess the accuracy of the theoretical techniques.

II. POTENTIAL-ENERGY CALCULATIONS

Our calculations on the MgH^+ system neglected all the spin-interaction terms in the Hamiltonian and assumed the Born-Oppenheimer separation of nuclear and electronic wave functions. Approximations to the electronic wave functions and energies were calculated using the configuration-interaction (CI) method. All calculations were performed using ALCHEMY, a system of programs for the calculation of molecular wave functions developed by Bagus, Liu, McLean, and Yoshimine at IBM-San Jose.

The Slater-type-function basis sets used in the MgH^+ calculations are given in Table I. The $7s$-$3p$ Mg basis of Clementi and Roetti[4] was augmented with $4s$, $3p$, and $3d$ functions that were optimized for the lowest self-consistent-field (SCF) energies of these atomic states. The hydrogen basis is exact through $n = 2$, with additional s, p, and d functions to provide flexibility for the molecular calculations.

The Mg basis yields an SCF energy for the Mg atom of $-199.614\,39$ hartrees, which is very close to the restricted Hartree-Fock value[5] of -199.6154 hartrees. The SCF dipole polarizability for Mg was calculated by a finite-perturbation method to be $80.3a_0^3$, while a fit to the long-range region of the $H^+ + Mg$ potential curve yielded a CI polarizability of $70.6a_0^3$. These values may be compared to the accepted value[6] from Reinsch and Meyer's atomic CI calculation[7] of $71.3a_0^3$. The H-atom

TABLE I. Slater-orbital basis set.

Mg	1s	12.323	H	1s	2.0
		19.548			1.0
	2s	4.439			0.5
		11.166		2s	0.5
	3s	0.897			0.333 333 33
		1.487		2p	1.0
		3.476			0.5
	4s	0.745			0.333 333 33
		1.863		3d	0.333 333 33
	2p	2.719			
		4.700			
		8.505			
	3p	0.765			
		1.070			
	3d	0.675			
		2.649			

basis yields the exact energies for the H(1s) and H($n=2$) states and produces an SCF dipole polarizability of $4.40a_0^3$, which may be compared with the exact value of $4.5a_0^3$.

In the CI calculations the core orbitals, K and L shells of Mg, were kept fully occupied and all single and double excitations of the two valence electrons were allowed. The CI calculations used

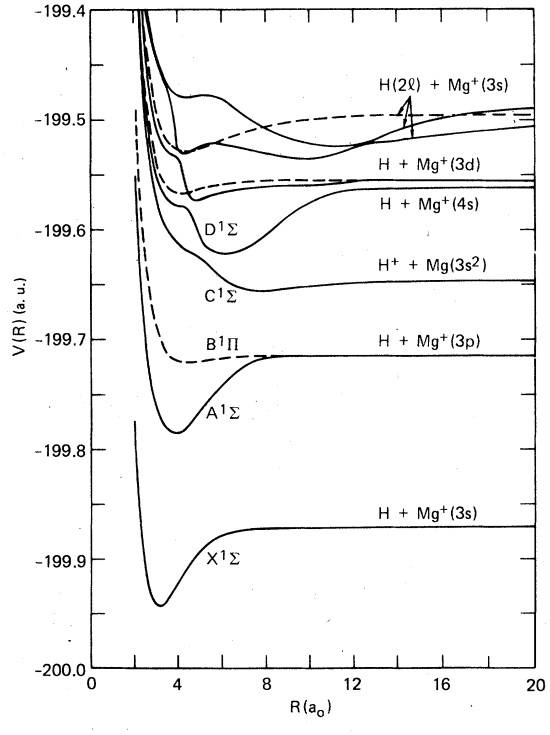

FIG. 1. CI potential energies for several low-lying singlet molecular states of MgH^+. The $^1\Sigma$ states are denoted by solid lines and the $^1\Pi$ states by dashed lines.

TABLE II. Representative values of the calculated potential energies for MgH^+ in units of hartrees (1 hartree = 27.212 eV, 199.0 hartrees has been added to each potential-energy value).

$R(a_0)$	$^1\Sigma_1(H+Mg^+)$	$^1\Sigma_2(H+Mg^+(3p))$	$^1\Sigma_3(H^++Mg)$	$^1\Sigma_4(H+Mg^+(4s))$	$^1\Sigma_5(H+Mg^+(3d))$	$^1\Sigma_6(H(n=2)+Mg^+)$	$^1\Sigma_7(H(n=2)+Mg^+)$	$^1\Pi_1(H+Mg^+(3p))$	$^1\Pi_2(H+Mg^+(3d))$	$^1\Pi_3(H(n=2)+Mg^+)$
2.0	−0.774 54	−0.551 61	−0.367 48	−0.342 61	−0.305 10	−0.246 65	−0.239 51	−0.490 89	−0.334 17	−0.292 46
2.5	−0.906 28	−0.701 54	−0.513 84	−0.491 50	−0.452 27	−0.392 33	−0.388 00	−0.634 20	−0.481 29	−0.439 44
3.0	−0.940 63	−0.761 25	−0.574 81	−0.551 40	−0.510 42	−0.450 42	−0.448 42	−0.691 39	−0.540 18	−0.499 22
3.25	−0.941 75	−0.774 76	−0.590 73	−0.565 19	−0.523 45	−0.464 21	−0.462 63	−0.704 91	−0.553 83	−0.513 58
3.5	−0.937 70	−0.781 95	−0.601 38	−0.573 02	−0.530 44	−0.473 09	−0.470 66	−0.712 95	−0.561 59	−0.522 16
3.75	−0.930 84	−0.784 75	−0.608 60	−0.577 04	−0.533 51	−0.502 63	−0.476 82	−0.717 47	−0.565 48	−0.526 91
4.0	−0.922 74	−0.784 44	−0.613 63	−0.578 78	−0.536 03	−0.528 76	−0.478 93	−0.719 77	−0.566 87	−0.529 14
4.25	−0.914 44	−0.781 90	−0.617 30	−0.579 72	−0.555 40	−0.531 43	−0.479 44	−0.720 68	−0.566 73	−0.529 72
4.5	−0.906 60	−0.777 74	−0.620 22	−0.584 09	−0.570 14	−0.529 41	−0.479 11	−0.720 77	−0.565 73	−0.529 22
5.0	−0.893 57	−0.766 47	−0.625 97	−0.607 89	−0.571 90	−0.524 61	−0.478 18	−0.719 82	−0.562 81	−0.526 38
6.0	−0.878 96	−0.741 75	−0.645 39	−0.622 30	−0.566 46	−0.522 23	−0.481 20	−0.717 33	−0.558 26	−0.518 32
7.0	−0.873 78	−0.725 07	−0.653 89	−0.617 38	−0.562 95	−0.526 95	−0.496 46	−0.715 81	−0.556 45	−0.511 18
8.0	−0.872 13	−0.717 86	−0.654 51	−0.603 92	−0.561 15	−0.531 61	−0.508 03	−0.715 06	−0.555 85	−0.505 98
9.0	−0.871 57	−0.715 45	−0.652 88	−0.588 16	−0.560 16	−0.534 65	−0.516 48	−0.714 70	−0.555 61	−0.502 12
10.0	−0.871 36	−0.714 69	−0.651 10	−0.574 65	−0.559 34	−0.535 15	−0.521 36	−0.714 50	−0.555 48	−0.498 98
30.0	−0.871 04	−0.714 19	−0.646 75	−0.561 92	−0.555 19	−0.499 77	−0.493 01	−0.714 19	−0.555 19	−0.495 92

TABLE III. Potential-curve characteristics.

State	D_e (eV) Calc.	D_e (eV) Spectroscopic [a]	NT [c]	$R_e(a_0)$ Calc.	$R_e(a_0)$ Spectroscopic [b]	NT [c]	ω_e (cm^{-1}) Calc.	ω_e (cm^{-1}) Spectroscopic [b]	B_e (cm^{-1}) Calc.	B_e (cm^{-1}) Spectroscopic [b]	T_0 (cm^{-1}) Calc.	T_0 (cm^{-1}) Spectroscopic [b]
$X^1\Sigma$	1.93	2.1	0.989	3.163	3.114	3.439	1639	1695	6.21	6.41	...	
$A^1\Sigma$	1.93	2.0	2.111	3.844	3.791	4.175	1090	1133	4.21	4.33	34220 (35469) [d]	35629
$B^1\Pi$	0.18	...	...	4.408	4.290	...	495	...	3.20	3.39	47990 (49326) [d]	49900

[a] From an RKR analysis of Numrich and Truhlar (Ref. 8).
[b] Spectroscopic values from Rosen (Ref. 9).
[c] Pseudopotential calculation of Numrich and Truhlar (Ref. 8).
[d] T_0 calculated from $E_{\text{spectro}}(Mg^+(3^2P) - Mg^+(3^2S)) + D_0(X^1\Sigma) - D_0(A^1\Sigma \text{ or } B^1\Pi)$.

an N-particle basis set of orthonormal-configuration-state functions constructed from the SCF occupied and virtual orbitals calculated on $MgH^{2+}(^2\Sigma)$. The dimensions of the CI calculations were 314 and 250 for the $^1\Sigma$ and $^1\Pi$ molecular states, respectively.

Potential points were calculated for 10 molecular states and 46 internuclear separations from $R = 2.0$ to $30a_0$. The results of these calculations are plotted in Fig. 1, but because of the large mass of data, only an abbreviated list of the numerical values is given in Table II. The potential-well characteristics of the three lowest states are given in Table III along with a comparison to spectroscopic data[8,9] and pseudopotential calculations.[8] The potential-well positions are in reasonable agreement with spectroscopic data ($\Delta R_e \leq 0.12a_0$), and the dissociation energies for the X and A states are within 10% of the values obtained in a RKR analysis by Numrich and Truhlar.[8] In Table III we also compare our CI calculations to the pseudopotential calculations of Numrich and Truhlar[8] who adjusted a polarization potential to best reproduce their RKR analysis on the $A\ ^1\Sigma$ state; the agreement is fair for the $A\ ^1\Sigma$ state but poor for the $X\ ^1\Sigma$ state.

We can also attempt to independently establish error limits on the $X\ ^1\Sigma$ and $A\ ^1\Sigma$ dissociation energies. Recently, we have completed extensive calculations on the NaH isoelectronic system where we have performed CI calculations with excitations from only the valence shell and also from both the valence- and L-electron shells. The inclusion of the core-valence correlation energies, as compared to the valence calculation, increased the dissociation energies of the $X\ ^1\Sigma$ and $A\ ^1\Sigma$ states by ~0.05 eV and decreased the equilibrium separations by $\sim 0.05a_0$. The best computed D_e are also within 0.02 eV of the spectroscopic values. Reinsch and Meyer[6] have shown that the core-valence correlation effects on dipole polarizability is greater for Na than Mg. Hence, for the isoelectronic MgH^+ system, our best estimate of the $X\ ^1\Sigma$ and $A\ ^1\Sigma$ dissociation energies is 1.98 eV, with conservative limits of ±0.05 eV. The $B\ ^1\Pi$ state is very weakly bound, Table III, and probably is uncertain by ±50%.

III. CROSS SECTONS

The low-energy electron-capture cross sections for reaction (1) were calculated using the A, C, and $D\ ^1\Sigma$ potential curves of Fig. 1. The potential curves indicate that the dominant products of the electron capture are the excited states $H + Mg^+(3p)$ and $H + Mg^+(4s)$. Three-state perturbed-stationary-state calculations employing straight-line

trajectories[10] were used along with the prescriptions derived by Melius and Goddard[11] (MG) to estimate the pertinent $\partial/\partial R$ radial coupling elements. As pointed out by MG, it is advantageous to use a molecular representation to describe the scattering process when there are more than two active channels.

In order to obtain the $\partial/\partial R$ parameters defined by MG, it is first necessary to construct diabatic potentials which are consistent with the adiabatic values. For our system, the A and C adiabatic molecular curves were decomposed to obtain a diabatic coupling matrix element H_{AC} by assuming diabatic A and C states which had the calculated $\Delta V(\infty)$ separation and employing a point-charge-induced dipole interaction ($\alpha_d/2R^4$) for the R dependence of the curves. The calculated dipole polarizabilities are given in Sec. II. We then obtained a H_{AC} whose exponential factor was $e^{-0.6R}$ in a.u. The region of maximum coupling, R_M, occurs at the location where $2H_{AC}(R) = \Delta V_{\text{diab}}(R)$. For this system, we find $R_M \approx 6.8a_0$. The analytical form[11] of this $\partial/\partial R$ matrix element is then given by

$$\left\langle A\left|\frac{\partial}{\partial R}\right|C\right\rangle = \frac{\beta}{2(e^{u}+e^{-u})}, \tag{4}$$

where $u = \beta(R - R_M)$ and β is the exponential decay factor $0.6a_0^{-1}$. Similarly, the $\partial/\partial R$ matrix elements between the C and D states around the avoided crossing at $R_x = 5.25a_0$ may be represented by[11]

$$\left\langle D\left|\frac{\partial}{\partial R}\right|C\right\rangle = \frac{0.5\alpha}{1+\alpha^2(R-R_x)^2}, \tag{5}$$

where $\alpha = \Delta F/\Delta V(R_x)$. ΔF is the absolute value of the difference in slopes of the diabatic potentials at R_x, and $\Delta V(R_x)$ is the adiabatic-potential separation at R_x. From the potential calculations, the $C-D$ parameter $\Delta V(R_x) = 0.0146$ hartree and the parameter ΔF was graphically determined to be 0.0338 hartree/a_0.

The three-state close-coupling calculations yield the cross sections depicted by the solid circles in Fig. 2. The calculations indicate that at the higher energies, $E \approx 5$–10 keV, electron capture into the $H + Mg^+(3p)$ state predominates. However, because of the large energy gap between the A and C states, production of $Mg^+(3p)$ decreases as the collision energy is lowered and coupling to the D and higher molecular states via the avoided crossings dominate. At the low energies we predict that the cross section will plateau around $\sim 1 \times 10^{-15}$ cm^2, which simply reflects the dimension of the repulsive wall of the potential where $\sigma = \pi R^2$ with $R \approx 3a_0$. Within this radius, several

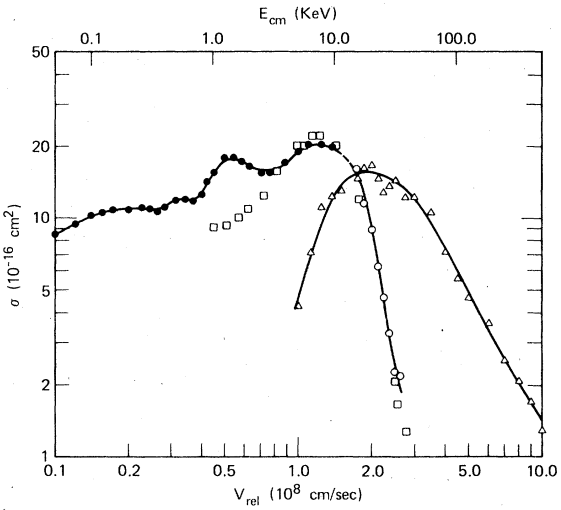

FIG. 2. Cross sections for $H^+ + Mg$ collisions. The solid circles are the single-electron-capture cross sections calculated in a three-state model using our potentials, whereas the open circles are the results of our Monte-Carlo calculations for this process; the open squares are the experimental data of Morgan and Eriksen (Ref. 2). The Monte-Carlo calculations for the impact-ionization process are denoted by the open triangles. Lines have been drawn through the calculated points as a visual aid.

electron-capture channels couple strongly to the initial state so it is reasonable to expect approximately unit probability for electron capture. The calculations also exhibit pronounced oscillatory structure that is due to an extremum in the difference of potential energies[12] at $R = 3a_0$ between the A and C states.

The experimental and calculated cross sections are found to be in very good agreement around the maximum at ~8 keV, indicating the A-C interaction has been reasonably accounted for. However, at lower energies the calculated values overestimate the electron capture; this indicates that states lying higher than the D states that populate simple excitation of the Mg atom will be important and must be accounted for in a more extensive (but very difficult) calculation. It should be noted that the experimental values tend to show the low-energy plateau predicted by the calculations, but there is no hint of any pronounced oscillatory structure.

The cross section calculations were extended into the atomic regime (region where the collision velocity is greater than the orbital velocity of the valence electrons, for Mg $v_e \approx 1.4 \times 10^8$ cm/sec) by means of the three-body three-dimensional (both nuclei and one active electron) classical-trajectory Monte Carlo method. This method has been fully

described previously.[13] For extension to the $H^+ + Mg$ collision system, an effective charge of 2.85, determined by using Slater's rules,[14] was used for the Mg nucleus, and the calculated cross sections were doubled to account for the two valence electrons. This latter approximation is valid because the transition probabilities are small and hence the unitarity of the S matrix is not severely violated.

The Monte Carlo electron-capture cross sections correlate well with the molecular results and also agree well with the experimental data, as shown in Fig. 2. In addition, impact-ionization cross sections are obtained simultaneously in the Monte Carlo calculation and are given by the open triangles in Fig. 2. At the highest velocities, the calculated impact-ionization cross sections also reflect electron removal from the L shell of Mg; this removal is significant and amounts to 50% of the cross section. The L-shell calculations employed an effective charge for the Mg nucleus of 7.85, again obtained from Slater's rules, with the calculated cross sections multiplied by 8 to reflect the equivalence of the L-shell electrons. The transition probabilities were small ($\lesssim 2\%$) and hence the unitarity of the S matrix was reasonably preserved. Unfortunately, there are no experimental data to compare with the ionization-cross-section calculations. Experience with Monte Carlo calculations on similar systems[15] indicates that the Monte Carlo cross sections will have a maximum uncertainty of $\pm 50\%$.

From Fig. 1 and crude Landau-Zener calculations we can predict the collision mechanism of double-electron capture to form H^- in $H^+ + Mg$ collisions, reaction (2). This cross section will be small, because of competition from single-electron excitation and transfer channels. The $H^- + Mg^{2+}$ channel is 8.3 eV endoergic and will be produced by two collision mechanisms. One mechanism is simply small-impact-parameter collisions that drive the particles up to the negative-ion state by the series of curve crossings between $R = 3$ and $5a_0$ on the repulsive wall of the potential. This mechanism will be important at high energies, because of the small-impact-parameter collisions required. The dominant mechanism at low energies will be the interaction of the $H^+ + Mg$ initial channel with the attractive $-2/R$ coulomb potential of the $H^- + Mg^+$ reactants. This is reflected in the adiabatic potentials by the avoided crossings between the C and D states at $5.25a_0$, another avoided crossing at $11a_0$ between the $H + Mg^+(3d)$ and $H(n=2) + Mg^+$ states, and the pinching together of the $^1\Sigma$'s arising from $H(n=2) + Mg^+$ at $12.5a_0$.

Using the C-D crossing and the $R = 11a_0$ crossing as the rate determining steps for double-electron capture, we have performed a crude three-state Landau-Zener calculation[16] to test our hypothesis. At 100 eV we obtain a cross section of 6.7×10^{-17} cm^2, which decreases to 3.1×10^{-17} cm^2 at 1000 eV. The latter number is in agreement with experiment[1] along with the energy dependence of the cross sections. Thus, as previously proposed,[3] the long-range attractive Coulomb potential of the reactants appears to determine the low-energy double-electron-capture process.

IV. CONCLUDING REMARKS

CI potential curves for the singlet molecular states of MgH^+ have been calculated and used in the calculation of the single-electron-capture cross section. This cross section is in reasonable agreement with experiment and indicates that the dominant products for collision energies between 50 and 10 000 eV are ground-state H and excited levels of Mg^+. Similarly, we can conclude from this study that the heavier alkaline earths will behave in the same manner with excited alkaline-earth ions and ground-state H preferentially produced after electron capture for $E \lesssim 10$ keV.

Monte Carlo calculations were performed for higher-energy collisions and the electron-capture cross sections are in good agreement with experiment. Impact-ionization cross sections are also presented, and the calculations at the highest energies indicate the importance of removal of L-shell electrons.

Low-energy, $E < 1$ keV, double-electron-capture cross sections were estimated using the CI potentials and confirm that the dominant collision process is population of the long-range $-2/R$ coulomb potential of the $H^- + Mg^{2+}$ products via an initial pseudo-curve-crossing with the $H^+ + Mg$ channel.

ACKNOWLEDGMENTS

The authors would like to thank Professor Morgan for releasing his experimental data before publication. This work was performed under a joint studies agreement between SRI and IBM. The work of one of us (R.E.O.) was supported by the U. S. Department of Energy under Contract No. E(04-3)-115, Project Agreement No. 111.

[1]T. J. Morgan and F. Eriksen, Phys. Lett. 66A, 198 (1978).
[2]T. J. Morgan and F. Eriksen, Phys. Rev. A 19, 1448 (1979).
[3]R. E. Olson, Phys. Lett. 55A, 83 (1975).
[4]E. Clementi and C. Roetti, At. Data Nucl. Tables 14, 177 (1974).
[5]C. F. Fischer, At. Data 4, 301 (1972).
[6]T. M. Miller and B. Bederson, Adv. Mol. Phys. 13, 1 (1978).
[7]E. A. Reinsch and W. Meyer, Phys. Rev. A 14, 915 (1976).
[8]R. W. Numrich and D. G. Truhlar, J. Phys. Chem. 79, 2745 (1975).
[9]B. Rosen, *Spectroscopic Data Relative to Diatomic Molecules* (Pergamon, New York, 1970), p. 254.
[10]A. Riera and A. Salin, J. Phys. B 9, 2877 (1976).
[11]C. F. Melius and W. A. Goddard, III, Phys. Rev. A 10, 1541 (1974).
[12]R. E. Olson, Phys. Rev. A 2, 121 (1970).
[13]R. E. Olson and A. Salop, Phys. Rev. A 16, 531 (1977).
[14]H. Erying, J. Walter, and G. E. Kimball, *Quantum Chemistry* (Wiley, New York, 1964), pp. 162 and 163.
[15]R. E. Olson, Phys. Rev. A 18, 2464 (1978).
[16]D. R. Bates and J. T. Lewis, Proc. Phys. Soc. A 68, 173 (1955).